



NIH PUBLIC ACCESS

Author Manuscript

*Chem Commun (Camb)*. Author manuscript; available in PMC 2014 July 18.

Published in final edited form as:

*Chem Commun (Camb)*. 2013 July 18; 49(56): 6313–6315. doi:10.1039/c3cc43620a.

## Glutathione-Complexed Iron-Sulfur Clusters. Reaction Intermediates and Evidence for a Template Effect Promoting Assembly and Stability

Wenbin Qi<sup>a</sup>, Jingwei Li<sup>b</sup>, C. Y Chain<sup>c</sup>, G.A. Pasquevich<sup>c</sup>, A. F. Pasquevich<sup>c</sup>, and J. A. Cowan<sup>a,b,\*</sup>

<sup>a</sup>Ohio State Biochemistry Program, The Ohio State University, 100 West 18th Ave, Columbus, OH 43210

<sup>b</sup>Department of Chemistry and Biochemistry, The Ohio State University, 100 West 18th Ave, Columbus, OH 43210

<sup>c</sup>Departamento de Física, Facultad de Ciencias Exactas, Universidad Nacional de La Plata, Argentina

### Abstract

Assembly and stabilization of a glutathione-complexed [2Fe-2S] cluster is promoted by aggregation of glutathione. The cluster core selects the tetramer species from a collection of equilibrating solution aggregate species, and in turn the core is stabilized toward hydrolytic degradation. Studies of glutathione derivatives, in combination with mass spectrometric and Mössbauer investigations provide insight on reaction intermediates during formation of [2Fe-2S] (GS)<sub>4</sub><sup>2-</sup>.

Glutathione is considered an important cellular redox buffering agent as a result of its high cellular concentration and low reduction potential.<sup>1</sup> Glutathione has also been implicated in cytosolic iron-sulfur cluster biosynthesis<sup>2,3</sup> with a recent study suggesting an essential role in cellular iron-sulfur cluster assembly, but only serving as a backup to thioredoxin for maintenance of cytosolic reduction potential.<sup>4</sup> The finding that glutaredoxins form an iron-sulfur cluster bridged dimer by incorporating two molecules of glutathione also supports the involvement of glutathione in cellular iron-sulfur cluster assembly pathways.<sup>5</sup> Previously we reported glutaredoxin to undergo cluster exchange with the scaffold protein ISU, consistent with glutaredoxin and glutathione playing a regulatory role in cellular iron-sulfur cluster assembly.<sup>3</sup> While small molecule iron-sulfur cluster compounds are typically stable only in non-nucleophilic solvents,<sup>6</sup> we have demonstrated the [2Fe-2S] core to be stabilized in aqueous solution following coordination by four molecules of glutathione.<sup>7</sup> The resulting cluster complex is stable at physiological pH and demonstrates exchange with the ISU scaffold protein.<sup>7</sup> Consequently we have proposed the glutathione iron-sulfur cluster

\*Corresponding author: [cowan@chemistry.ohio-state.edu](mailto:cowan@chemistry.ohio-state.edu).

†Electronic Supplementary Information (ESI) available: Experimental details concerning the synthesis and characterization of glutathione derivatives, and NMR, Mössbauer and ESI-MS experiments. See DOI: 10.1039/b000000x/

complex to be a potential substrate candidate for the mitochondrial ABC7-type iron-sulfur cluster exporter, as well as a component of the cellular labile iron pool.<sup>7, 8</sup>

Herein we evaluate the solution factors that promote the formation and stability of the glutathione-stabilized Fe-S cluster. These studies suggest a natural template effect, similar to the function of a dynamic combinatorial library, where the assembling cluster selects from an equilibrating pool of glutathione aggregates that in turn are stabilized by intermolecular salt-bridge formation. Furthermore, we describe the detection of the glutathione-complexed Fe-S cluster and reaction intermediates, the evolution of iron oxidation state, and kinetics of formation of this complex by a novel application of mass spectrometric and Mössbauer techniques.

The glutathione iron-sulfur cluster complex was synthesized by mixing reduced glutathione, ferric ion and sulfide in water at pH 8.6.<sup>9</sup> Formation of this cluster complex was evidenced by electronic absorption, NMR, Mössbauer and electrochemical experiments.<sup>9</sup> Mass spectrometry was also demonstrated to be a valuable aid in cluster characterization. Although several iron-sulfur cluster proteins have been studied by ESI-MS the general instability of non-protein-bound iron-sulfur cluster compounds has rendered the characterization of these small complexes by mass spectrometry to be challenging and very rare.<sup>10</sup> Nevertheless, when the reaction mixture described herein was analyzed by ESI-MS (Fig. 1) an exact mass peak at  $m/z=1425.3$  is clearly observed that is consistent with a cluster carrying two ferric ions,  $[(GS^-)_4[2Fe-2S]^{2+}+2H^++Na^+]^+$ . Exchange with  $K^+$  results in the expected mass shifts (Fig. S6). The peaks observed at 1405.3 and 1427.3 in Fig. 1 correspond to aggregates of glutathione in the reaction mix. Aggregation is discussed later in the paper and provided important insight on the factors that promote the stability of a complex that should not be stable, based on prior literature precedent for ligand complexes of iron-sulfur centers.

The intensities of the peaks at 1425.2 and 1426.3 (Fig. 1) were observed to increase as the reaction continued. In the theoretical isotopic distribution profile, the pure oxidized complex has the ratio 0.48. Thus, the exact mass peak at  $m/z=1426.3$  represents both an isotopic peak from the oxidized complex as well as the mixed valence complex  $[(GS^-)_4[2Fe-2S]^+ + 3H^+ + Na^+]^+$ . Based on the theoretical peak intensity ratio, we were able to deconvolute the intensities of peaks at 1425 and 1426 and calculate the actual intensity of bis-ferric  $Fe^{3+}/Fe^{3+}$  and mixed valence  $Fe^{3+}/Fe^{2+}$  species, respectively. By plotting calculated peak intensity versus time and fitting to first order exponential kinetics, the observed reaction rate constants for the formation of each of the  $Fe^{3+}/Fe^{3+}$  and  $Fe^{3+}/Fe^{2+}$  species are  $0.16 \pm 0.03 \text{ min}^{-1}$  and  $0.34 \pm 0.10 \text{ min}^{-1}$ , respectively (Fig. 2).

It is clear that after an initial phase, the solution quickly reaches an equilibrium in which there is a steady-state ratio of fully oxidized cluster (species I signals) and mixed valence cluster (species II and III signals). When a sample of reaction solution is ethanol precipitated and the solid material then analysed by Mössbauer spectroscopy, both the mixed valence  $Fe^{3+}/Fe^{2+}$  and fully oxidized  $Fe^{3+}/Fe^{3+}$  cluster species are evident (Fig. 2, right). Isomeric and quadrupolar shifts of III agree with literature values of ferric iron in the reduced 2Fe-2S cluster.<sup>11-14</sup> The fitted spectra also indicated an equimolar ratio of species II and III, and

support the identity of the one-electron reduced diiron cluster. Mössbauer experiments show that when the freshly synthesized cluster complex is isolated by ethanol precipitation and redissolved with excess glutathione then only fully oxidized cluster is present, exhibiting the NMR and other physical characteristics of the  $[2\text{Fe}-2\text{S}](\text{GS})_4^{2-}$  cluster.<sup>9</sup> These results indicate that while the fully oxidized cluster is the most stable solution state for the cluster, the conditions of the initial reaction mixture (with excess iron and sulphide and thiols) maintain a thermodynamic fraction of reduced cluster.

The major difference between the solid-state and solution spectra is species II (Table 1) which shows a feature with  $\delta \sim 1.10$  mm/s that is assigned to either a five or six coordinate  $\text{Fe}^{2+}$  center in the mixed-valent cluster based on similarity to published data, allowing for differences in sample temperature.<sup>15-18</sup> Moreover, the Gaussian standard deviation sigma of the interaction corresponding to  $\text{Fe}^{2+}$  is larger than the other peaks, showing that the atomic arrangement around  $\text{Fe}^{2+}$  is less defined. Expanded coordination reflects both the larger HS ferrous ion and the presence of an intramolecular chelate effect through carboxylate ligation from one or two  $\alpha$ -carboxylates on two glutamate residues (Fig. 3), and is consistent with prior reports of ferrous centers in binuclear iron<sup>15-18</sup> as well as proton relaxation studies that indicated the glutamate side chains to lie in close proximity to the cluster center.<sup>7</sup> Significantly, carboxylate coordination does not impact the expected  $m/z$  values in ESI-MS experiments.

The mass spectral peaks at 1413.3 and 1435.3 (Fig. 1) correspond to an intermediate species, which has a cluster center of  $[2\text{Fe}^{3+}-\text{S}^{2-}]$  with four coordinated molecules of glutathione. This species is most likely an intermediate formed on the reaction pathway because cluster alone does not yield these peaks. A recent report described an intermediate cluster assembly product, in a complex of the sulfur donor and cluster scaffold proteins (IscS-IscU) with fully oxidized iron and a related bridging persulfide ( $\text{Fe}_2\text{S}-\text{S}^-$ ) adduct.<sup>19</sup> Accordingly, the  $[(\text{GS}^-)_4][2\text{Fe}^{3+}-\text{S}^{2-}]$  species that we observe could represent an intermediate awaiting delivery of the second sulfide to complete the cluster core.

Crystallographic studies have earlier revealed a hydrogen bond network in crystals of glutathione<sup>20</sup> and it is of significant interest that a solution of glutathione by itself shows evidence of substantial aggregation, with trimers, tetramers, pentamers, etc ..., that are clearly visible in mass spectra (Fig. 4); especially in the lower  $m/z$  range where such aggregates are better distinguished from the sodium adducts exhibited in Fig. 1 (top). The  $(\text{GSH})_4$  tetramer is the most abundant species evident in Fig. 4. Aggregation is essentially eliminated by carboxyl ester formation or amine acetylation, respectively (Fig. 4 versus Figs. S4 and S5), while increasing ionic strength also yields the pronounced decrease in cluster stability (Fig. S7) that is expected when the salt bridges are disrupted. Fig. 3 illustrates a likely intermolecular salt bridge/H-bonding network for glutathione tetramer that appears to be of the correct size to serve as a preassembled iron-sulfur cluster chelate, ready to accept free iron and sulfide to form the stable cluster complex. No other glutathione aggregates are observed in the presence of cluster. Apparently there is a synergic interaction with the tetramer species selected by the cluster core, which in turn is stabilized by the glutathione aggregate. Through hydrogen bonding and salt-bridge formation, glutathione

forms an apparent tetrameric macrocycle that stabilizes and promotes formation of the iron-sulfur cluster complex.

## Conclusions

Characterization of small molecule iron-sulfur cluster complexes in aqueous solution has proven to be a challenge as a result of the hydrolytic instability. Herein we have obtained experimental support for a hypothesis that explains the stability associated with glutathione-complexed iron-sulfur complexes. In particular, the propensity of glutathione to aggregate, apparently through intermolecular salt bridge and hydrogen bond formation, yields a pre-assembled tetrameric species that forms a stable binding pocket for a [2Fe-2S] cluster core. Moreover, it was possible to identify certain reaction intermediates and monitor the kinetics of cluster formation by ESI-MS and Mössbauer experiments. The formation of glutathione iron-sulfur cluster complex was confirmed by the appearance of exact mass peaks at 1425.3 and 1426.3, which correspond to fully oxidized and mixed valence species, respectively. Reaction kinetics was studied by following peak intensities in ESI-MS spectra and apparent first order reaction constants were obtained. The structural model that we propose can be viewed as nature's equivalent of a dynamic combinatorial selection experiment from a pool of equilibrating glutathione oligomers. In this case a [2Fe-2S] core selectively binds and stabilizes a tetrameric macrocyclic aggregate, and in turn is stabilized toward hydrolysis.

## Supplementary Material

Refer to Web version on PubMed Central for supplementary material.

## Acknowledgments

This work was supported by a grant from the National Institutes of Health [AI072443].

## Notes and references

1. Pompella A, Visvikis A, Paolicchi A, De Tata V, Casini AF. *Biochem Pharmacol.* 2003; 66:1499–503. [PubMed: 14555227]
2. Sipos K, Lange H, Fekete Z, Ullmann P, Lill R, Kispal G. *J Biol Chem.* 2002; 277:26944–9. [PubMed: 12011041]
3. Qi W, Cowan JA. *Chem Commun (Camb).* 2011; 47:4989–91. [PubMed: 21437321]
4. Kumar C, Igbaria A, D'Autreaux B, Planson AG, Junot C, Godat E, Bachhawat AK, Delaunay-Moisan A, Toledano MB. *EMBO J.* 2011
5. Johansson C, Kavanagh KL, Gileadi O, Oppermann U. *J Biol Chem.* 2007; 282:3077–82. [PubMed: 17121859]
6. Enemark JH, Cooney JJ, Wang JJ, Holm RH. *Chem Rev.* 2004; 104:1175–200. [PubMed: 14871153]
7. Qi W, Li J, Chain CY, Pasquevich GA, Pasquevich AF, Cowan JA. *J Am Chem Soc.* 2012; 134:10745–8. [PubMed: 22687047]
8. Kuhnke G, Neumann K, Muhlenhoff U, Lill R. *Mol Membr Biol.* 2006; 23:173–84. [PubMed: 16754360]
9. Qi W, Li J, Chain CY, Pasquevich GA, Pasquevich AF, Cowan JA. *J Am Chem Soc.* 2012
10. Rao PV, Holm RH. *Chemical Reviews.* 2004; 104:527–559. [PubMed: 14871134]

11. Munck E, Debrunner PG, Tsibris JCM, Gunsalus IC. *Biochemistry*. 1972; 11:855–863. [PubMed: 4333945]
12. Dunham WR, Bearden AJ, Salmeen IT, Palmer G, Sands RH, Orme-Johnson WH, Beinert H. *Biochim Biophys Acta*. 1971; 253:134–152. [PubMed: 4331269]
13. Anderson RE, Dunham WR, Sands RH, Bearden AJ, Crespi HL. *Biochim Biophys Acta*. 1975; 408:306–318. [PubMed: 172131]
14. Meyer J, Clay MD, Johnson MK, Stubna A, Münck E, Higgins C, Wittung-Stafshede P. *Biochem*. 2002; 41:3096–3108. [PubMed: 11863449]
15. Zheng YZ, Xue W, Tong ML, Chen XM, Grandjean F, Long GJ. *Inorg Chem*. 2008; 47:4077–4087. [PubMed: 18422310]
16. Yoon S, Lippard SJ. *J Am Chem Soc*. 2005; 127:8386–8397. [PubMed: 15941272]
17. Paredes-García V, Venegas-Yazigi V, Latorre RO, Spoding E. *Polyhedron*. 2006; 25:2026–2032.
18. Burns RG. *Hyperfine Interactions*. 1994; 9:739–745.
19. Marinoni EN, de Oliveira JS, Nicolet Y, Raulfs EC, Amara P, Dean DR, Fontecilla-Camps JC. *Angew Chem Int Ed Engl*. 2012; 51:5439–42. [PubMed: 22511353]
20. Wright WB. *Acta Cryst*. 1958; 11:632–642.

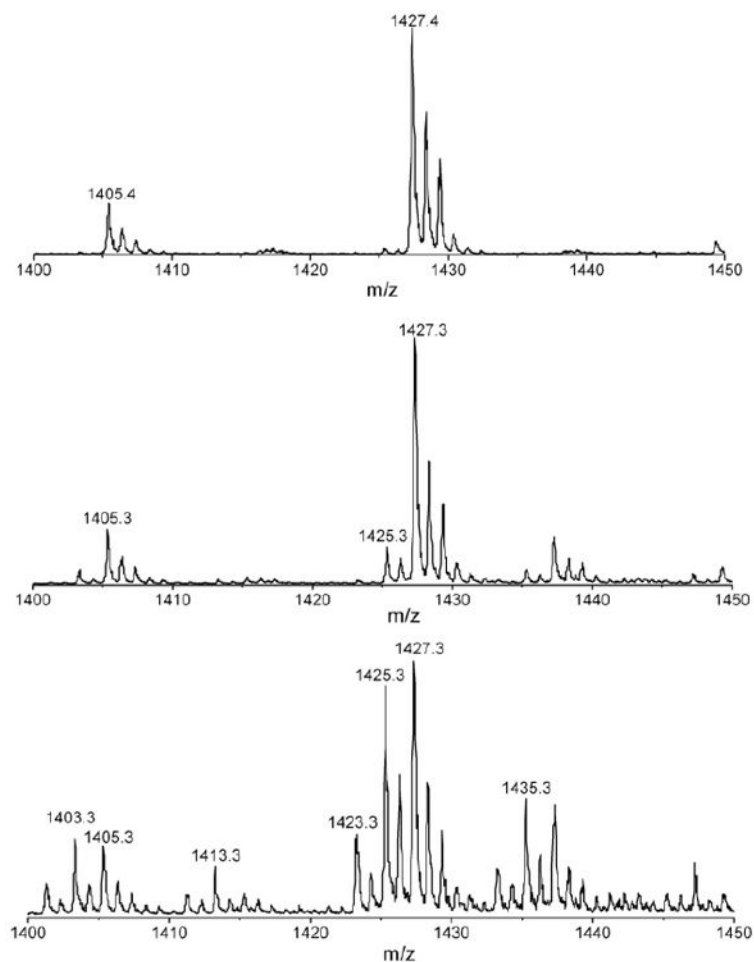


**Fig. 1.**

Analysis of  $[2\text{Fe-2S}](\text{GS})_4$  formation by ESI mass spectrometry. (Top) ESI-MS of GSH buffer solution at pH 8.6, showing exact mass peaks at 1405.3 and 1427.3, corresponding to the glutathione tetramer species,  $[(\text{GS}^{2-})_4 + 8\text{Na}^+ + \text{H}^+]^+$  and  $[(\text{GS}^{2-})_4 + 9\text{Na}^+]^+$ , respectively, each with a deprotonated thiol and carboxyl ( $\text{GS}^{2-}$ ). (Middle) ESI-MS of a reaction mixture of GSH,  $\text{Fe}^{3+}$ , and  $\text{S}^{2-}$  at 2 min. The exact mass peak at  $m/z=1425.3$  is consistent with  $[(\text{GS}^-)_4[2\text{Fe-2S}]^{2+} + 2\text{H}^+ + \text{Na}^+]^+$  where  $\text{GS}^-$  is the thiolate form of glutathione, and the peak at  $m/z=1426.3$  is consistent with both  $[(\text{GS}^-)_4[2\text{Fe-2S}]^+ + 3\text{H}^+ + \text{Na}^+]^+$  and an isotopic peak of  $[(\text{GS}^-)_4[2\text{Fe-2S}]^{2+} + 2\text{H}^+ + \text{Na}^+]^+$ . (Bottom) ESI-MS of the reaction mixture of GSH,  $\text{Fe}^{3+}$ , and  $\text{S}^{2-}$  at 24 min. Exact mass peaks at both  $m/z=1425.3$  and  $m/z=1426.3$  are greater, showing the formation of the cluster in both bis-ferric  $\text{Fe}^{3+}/\text{Fe}^{3+}$  and mixed valence  $\text{Fe}^{3+}/\text{Fe}^{2+}$  forms.

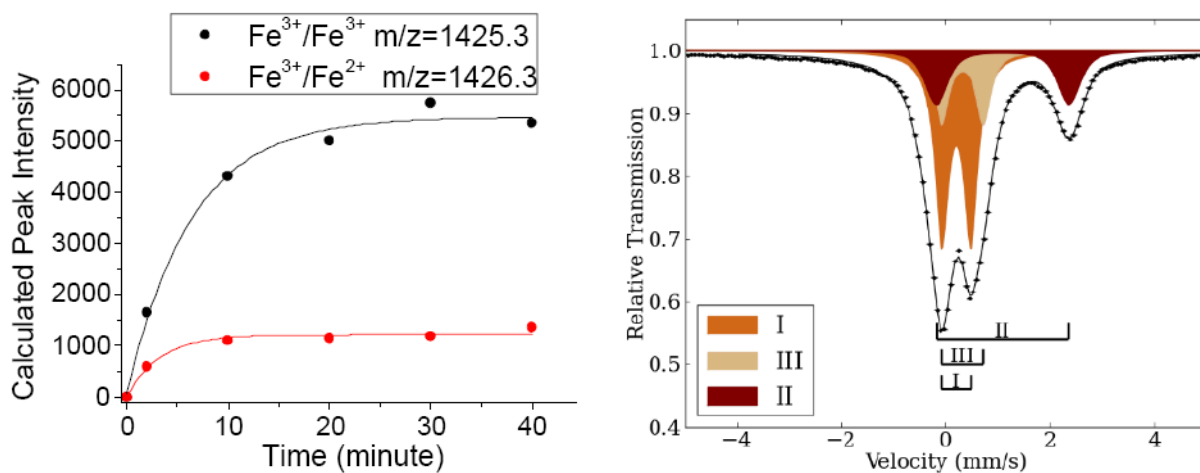


**Fig. 2.**

(left) Plot of the peak intensity of the mixed valence  $\text{Fe}^{3+}/\text{Fe}^{2+}$  form at  $m/z=1425.3$ , and the  $\text{Fe}^{3+}/\text{Fe}^{3+}$  form at  $m/z=1426.3$ , versus reaction time; (right) Mössbauer spectrum of the isolated cluster in the solid-state recorded at room temperature. The solid line corresponds to the fitting curve. In order to better visualize the three interactions, their contribution to the mean nuclear cross section are presented as colored peaks (see SI for more details on the interactions and the relation between the absorption cross section and the absorption profile - the fitting curve).

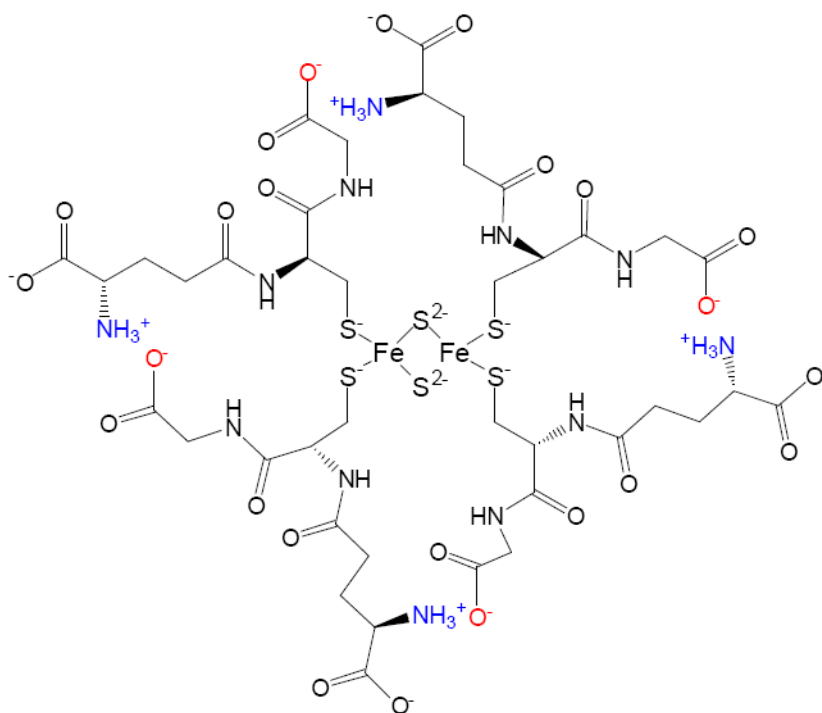


**Fig. 3.**

A two-dimensional representation of a glutathione-complexed cluster aggregate. Salt bridge formation between carboxylates and protonated amines appear to favor aggregation of glutathione and is supported by the ionic strength dependence of cluster stability (Fig. S7) and the effect of acetylation and esterification that effectively eliminate multimer formation (Figs. S4 and S5). In glutathione solutions the tetrameric oligomer is the most abundant species, as reflected by mass spectra (Fig. 4) and appears to create a pocket for cluster binding that is optimal in size, relative to other aggregate forms. Presumably this pocket mimics a protein binding site by both providing a pre-assembled ligand set, as well as providing a measure of protection from solvent access in the folded state.



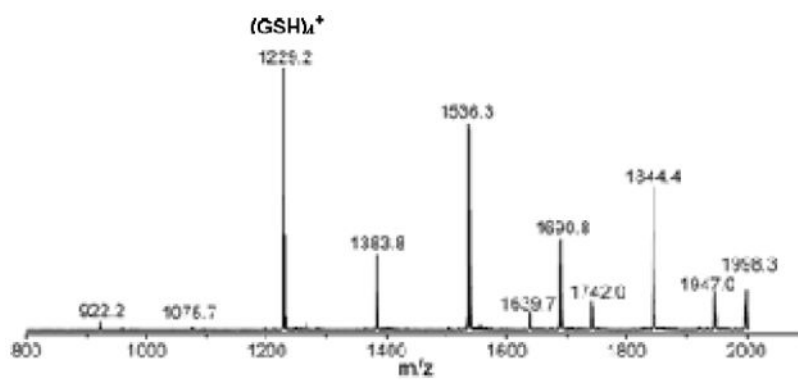


**Fig. 4.** Solution aggregates of glutathione observed by ESI-MS, with evidence of trimers, tetramers, pentamers, etc ... formation. These solutions were not pH adjusted with NaOH and do not show the Na<sup>+</sup> adducts evident in Fig. 1 (top).

**Table 1**

Mössbauer parameters of solid-state form cluster and assigned oxidation states and geometry.

Species	Contribution	$\delta$ (mm/s)	$\Delta E_Q$ (mm/s)	Identity	Geometry
I	56±1 %	0.21±0.02	0.55±0.03	Fe <sup>3+</sup>	4-coord, T <sub>d</sub>
II	23±1 %	1.10±0.04	2.54±0.08	Fe <sup>2+</sup>	5- or 6-coord
III	21±1 %	0.33±0.02	0.79±0.03	Fe <sup>3+</sup>	4-coord, T <sub>d</sub>